PREDICTION OF HEAT TRANSFER FOR A FILM COOLED FLAT PLATE USING A COMPUTATIONAL FLUID DYNAMICS ANALYSIS

A THESIS

Presented in Partial Fulfillment of the Requirements for Graduation with Distinction in Mechanical Engineering of The Ohio State University

By

Timothy M. Schroeder

****

The Ohio State University
2009

Thesis Examination Committee:
Professor Michael G. Dunn, Advisor
Professor Mohammad Samimy

Approved by

_____
Advisor

Undergraduate Program in Mechanical Engineering

ABSTRACT

It has become common practice within the gas turbine industry to simulate the flow of the primary air stream and cooling gas by using the numerical method associated with Computational Fluid Dynamics (CFD). A variety of CFD programs exist in the commercial market today and within the proprietary industry environment. While most can predict the aerodynamics inside engine turbines, the ability to predict heat transfer for a film-cooled turbine stage remains elusive. The purpose of this project was to benchmark the current state of heat transfer prediction for commonly used CFD software. The commercially available code FINE/Turbo, developed by Numeca International, was tested in this research effort. FINE/Turbo was used because of its ability to provide time-accurate solutions, which will be utilized in future research efforts.

The computational model utilized a conjugate heat-transfer model for solid-fluid interactions, as well as 113 individual cooling holes spaced consistent with the turbine blade hardware. Current heat-transfer solutions are in the expected range of theoretical values, although the measurement program is still in process. The addition of cooling flow to the mainstream flow associated with a high-pressure turbine stage is difficult to model, especially when one is attempting to predict the surface heat-transfer rate. Boundary layer conditions and solid-fluid interactions dominate the region, making accurate computational predictions very difficult. Results of this project have identified areas for which improvement in the current state-of-the-art are required, and have provided a benchmark for computational solutions. Lessons learned from the flat-plate measurement program will be applied to a full-scale rotating turbine stage in the near future, so understanding how to predict the local heat transfer using the CFD code is of significant interest.

ACKNOWLEDGEMENTS

This project could not have happened without the constant advice, support, and encouragement of the people at the Ohio State Gas Turbine Laboratory (GTL). In particular, I would like to thank my advisor, Dr. Michael Dunn, for his knowledge and direction throughout the project. I would also like to thank PhD student Randy Mathison, who was an invaluable help for solving the day-to-day challenges of CFD software.

A mention of thanks is due to Sam Kheniser for his assistance in providing necessary information about the wind tunnel experiments. Finally, I would like to thank Mark Wishart for his ongoing suggestions and comments on CFD simulations.

VITA

1985……. Born- Bowling Green, Ohio

2004- Present…….. B.S. Mechanical Engineering, The Ohio State University

FIELDS OF STUDY

Major Field: Mechanical Engineering

TABLE OF CONTENTS

LIST OF FIGURES

LIST OF TABLES

NOMENCLATURE AND ABBREVIATIONS

NOMENCLATURE

CFD	Computational Fluid Dynamics
IGG	Interactive Grid Generator (part of FINE/Turbo)
OSU GTL	Ohio State Gas Turbine Laboratory
S-A	Spalart-Allmaras turbulence model
SCF	Small Calibration Facility

ABBREVIATIONS

c	Speed of sound
$\bar{h}$	Heat transfer coefficient
k_{air}	Thermal conductivity of air
k_{al}	Thermal conductivity of 6061-T6 aluminum
L	Plate length
$\dot{m}_a$	Mass flow of free-stream air
$\dot{m}_c$	Mass flow of cooling air
Ma	Mach number
$\overline{Nu}$	Nusselt number
P_o	Outlet pressure
P_s	Supply tank pressure
Pr	Prandtl number
q	Heat flux
R	Specific gas constant
Re	Reynolds number

T_{cool}	Cooling gas temperature
T_i	Inlet temperature
T_t	Total temperature
T_s	Static temperature
V	Flow velocity
y^+	Non-dimensional wall distance
γ	Adiabatic index
ΔT	Temperature difference
μ	Dynamic viscosity
ρ	Air density

Chapter 1
THE RESEARCH PROGRAM AND BACKGROUND INFORMATION

1.1 Introduction to Turbine Cooling

The dramatic increase of computing power in the last 20 years has revolutionized thermal and fluid science, paving the way for full-scale turbine simulations using Computational Fluid Dynamics. CFD predictions of turbine aerodynamics have recently become quite accurate, allowing for a quicker and more robust design of jet engine turbines [2]. Predicting heat transfer for film-cooled turbines, however, remains a difficult and arduous task, which continues to slow and hamper turbomachine development. Compounding this dilemma is the industry's ceaseless drive to increase engine efficiency, primarily accomplished by raising the inlet temperature of hot gasses to the turbine from the combustor [3]. In many applications, inlet temperatures are at or above the melting point of the metal from which the turbine blades are constructed. Moreover, combustor exit non-uniformities such as turbulence and hot streaks can lead to unbalanced heat loads in the turbine, resulting in high levels of thermal stresses ultimately ending in blade failure [4].

In order to avoid catastrophic thermal failure in the turbines, a variety of innovative techniques have been employed, including coating turbine airfoils with special thermal barriers and introducing a thin film of coolant air over the airfoils for protection from the devastating effects of hot combustion gasses [5]. This addition of coolant air has become common practice in high-performance engines, but since the air is traditionally extracted from the compressor stage, a decrease in thermodynamic cycle efficiency results [6]. Thus, it is advantageous to bleed only the optimal amount of air in order to maintain efficiency while still cooling the airfoils.

The sophisticated geometry and complex aerodynamic flows of turbine airfoils are frequently modeled in industry as flat plates to simplify calculations and reduce costs. Flat-plate models reduce instrumentation and design difficulties while still providing accurate and useful data, resulting in quicker experiment setup times. The flat-plate used in this project is a flattened version of an actual turbine blade, retaining commonality in the critical area of cooling hole geometry. Previous research on film cooling and heat transfer has focused primarily on the fundamental physics of the problem and instrumentation of turbines [1]. As a result, comparing results of flat plate models to the current state of CFD software is still both novel and useful.

1.2 Research Objectives

The goal of this research effort was to investigate the accuracy of computer simulations by comparing numerical results against experimentally obtained data in determining heat transfer. The ability to accurately predict heat transfer in gas turbines is of extreme importance to engine manufacturers, as areas that are too hot will quickly develop failure-inducing thermal stresses [7]. In addition to potentially reducing breakage and failure, accurate predictions of thermal properties can save substantial costs through the reduction of engine design time.

The CFD software package FINE/Turbo, developed by NUMECA International, was selected for the computational portion of this project. Although a number of other commercially available CFD codes exist on the market today, FINE/Turbo was selected because of its specialization in turbomachinery applications and its ability to solve a wide variety of aerodynamic and thermal problems. In addition, FINE/Turbo is able to provide time-accurate solutions. Although time-accurate cases were not simulated in this research effort, future work at the GTL will utilize this feature for obtaining the heat transfer of turbine blades in a full scale

rotating rig. Thus, the insights and best practices obtained by this project will directly impact future research work. This project is the first heat transfer CFD work of its kind done at the GTL, so by utilizing a flat plate model much insight was gained into the details and nuances of CFD heat transfer.

FINE/Turbo operates by solving the Reynolds Averaged Navier-Stokes equations in either two or three dimensions. In order to accurately simulate the experimental flow conditions, the three dimensional solver was required, at the expense of significantly more time and computational power.

Numeca International's FINE/Turbo package contains a complete family of software tools for solving Computational Fluid Dynamics problems. All pre-processing and post-processing activities were carried out in FINE/Turbo, for both ease of use and to avoid computational difficulties arising from transferring files between programs. The software IGG (Interactive Grid Generator), part of FINE/Turbo, was used to create the geometric shapes used in this research project. IGG is setup in 3D Cartesian coordinates, which made it an obvious choice for this project. The grid meshing steps also took place in IGG.

Boundary conditions and initial solutions were chosen in FINE/Turbo's main interface, which is able to read data directly from the IGG mesh. When the model was ready, the program FINE/Euranus was run to solve the computational problem. Finally, the FINE software CFView was used for post-processing and prediction evaluation.

Chapter 2
EXPERIMENTAL SETUP

2.1 Small Calibration Facility

The CFD simulations of this project were designed to model the real-world experiments conducted in the Small Calibration Facility (SCF) at the OSU GTL. A short description of the SCF and its operation has been included to provide some background information.

The SCF operates as a medium-duration blow-down facility, which is used for both instrument calibration and as a small test facility [5]. In this experimental investigation, the SCF was utilized in its small test facility capacity. A photograph of the SCF and a schematic are included below as Figures 1 and 2.

Figure 1: Photograph of the Small Calibration Facility

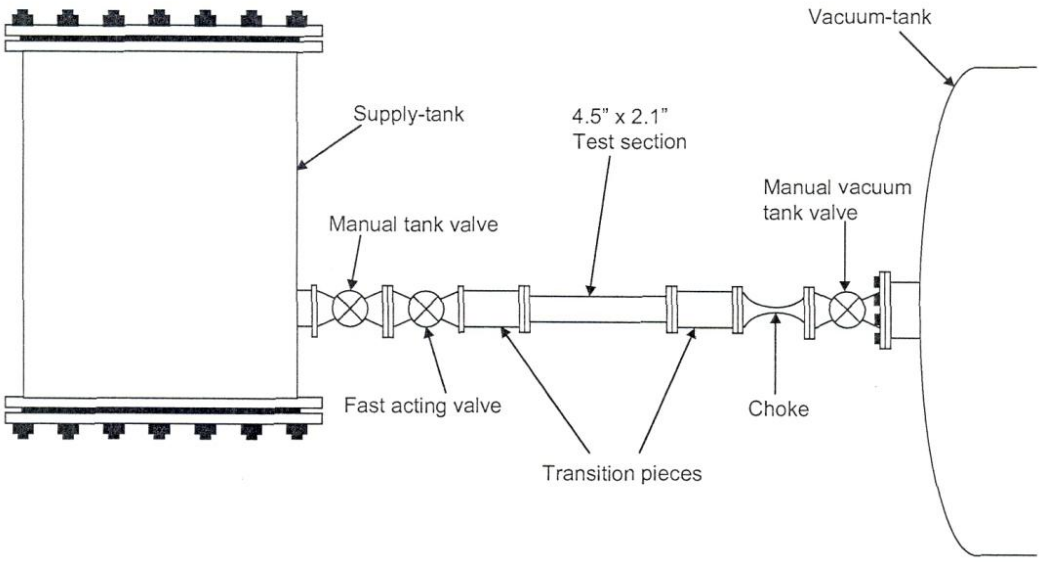

Figure 2: Schematic of the Small Calibration Facility [5]

The SCF runs as blow-down wind tunnel, with subsonic flow through the 4.5" x 2.1" test section, flow of Mach 1 at the choke, and supersonic flow on the vacuum-tank side of the choke. A 0.71 m^3 supply tank provides heated and pressurized air to the test section, where the instrumented flat-plate used in the experiment is located. The air inside the supply tank is mixed using an internal fan, and is insulated from the outside with fiberglass insulation. Thus, the air inside the supply tank can be considered homogenous in both temperature and pressure.

Flow is initiated by opening the fast-acting valve, a computer-controlled valve which allows data collection to begin at exactly the same time airflow starts [5]. The test section and vacuum-tank are initially void of air, so when the fast-acting valve opens a rush of unsteady air enters the system. After a short time, the unsteady conditions change to steady conditions. It is in the steady regime of the wind tunnel that is most interesting to this experimental effort. Figure

3 below shows a picture of the test section, while Figure 4 shows a CAD model of the same section.

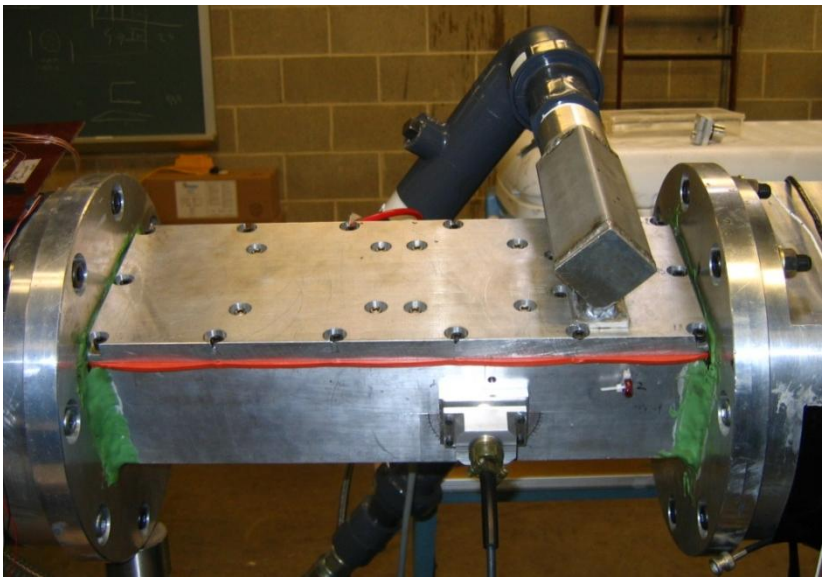

Figure 3: Test Section Containing Flat Plate

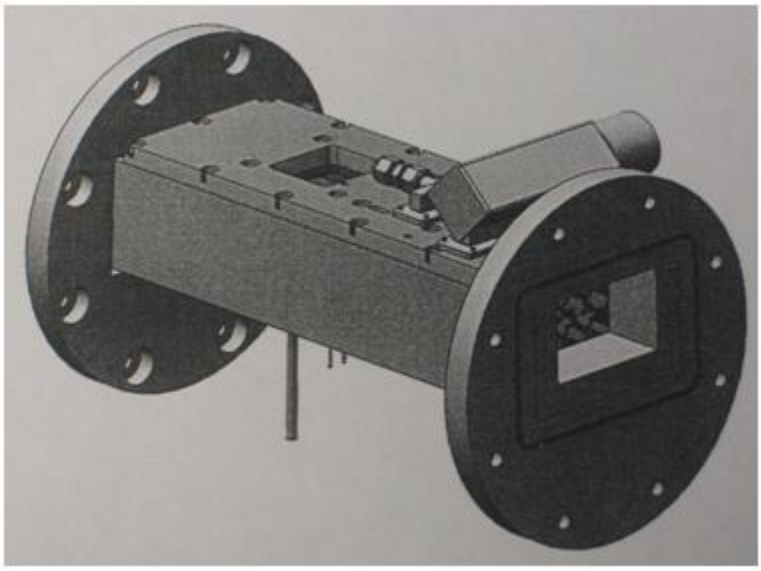

Figure 4: CAD Model of the Test Section [5]

A turbulence grid was installed between the supply tank and the test section to provide a uniform turbulent flow pattern into the test section. In addition, a 2.76 in. diameter choke was used to accelerate the air flow to a desired mach number of 0.4 in the test section.

The test plate was divided into four sections: a boundary layer bleed, a turbine blade plate, a turbine vane plate, and an exit flow section. For this research effort, the turbine blade plate is of primary interest. The turbine blade plate was instrumented with two rows of double-sided Kapton heat-flux gauges, which were developed in-house at the OSU GTL. Figure 5 shows the location of these gauges on the plate.

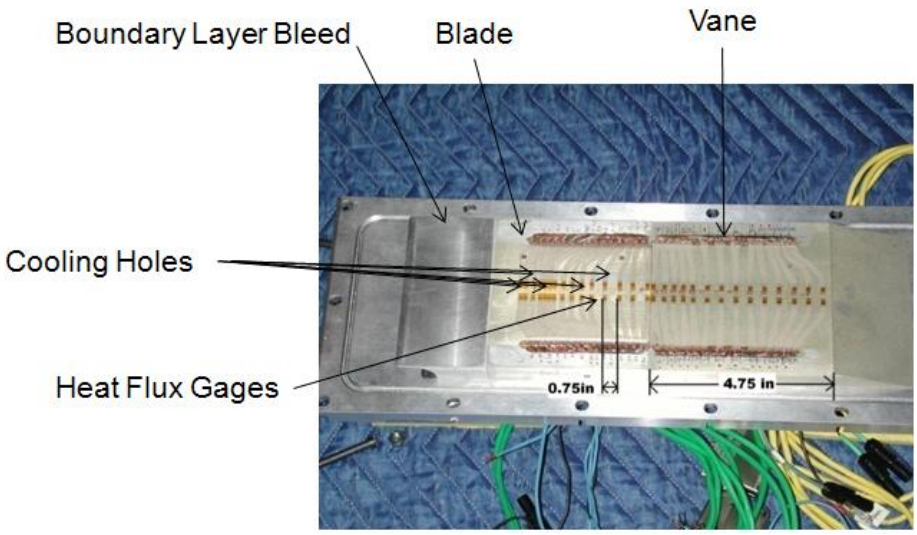

Figure 5: Instrumented Flat Plate

All of the instrumentation associated with the experiment was fed through a newly designed Data Acquisition Board, and into a central computer for reduction and analysis in LabVIEW. The collection and reduction of experimental data were carried out by Sam Kheniser as part of a separate MS Thesis program at the OSU GTL.

2.2 Boundary Conditions

The boundary conditions used in the CFD simulations were modeled after the flat plate experiments of the SCF. Table 2.1 summarizes the given boundary conditions, while Table 2.2 shows the boundary conditions that required further calculations using the given values.

Table 1: Given Test Section Boundary Conditions

Ma	Inlet Mach Number	0.4
T_s	Inlet Static Temperature	470 K
T_{cool}	Cooling Gas Temperature	240 K
P_s	Supply Tank Pressure	517.1 kPa
$\dot{m}_c$	Cooling Mass Flow	0.006 kg/s
k_{al}	6061-T6 Thermal Conductivity	177 W/mK

Table 2: Calculated Test Section Boundary Conditions

c	Speed of Sound	433 m/s
V	Flow Velocity	173 m/s
Po	Outlet Pressure	463.13 kPa
$\dot{m}_a$	Air Mass Flow (theoretical)	3.66 kg/s

The Mach number, supply tank pressure, cooling gas temperature, and inlet temperature were provided for this experiment. The cooling mass flow and thermal conductivity were also assumed to be given values in this experiment. However, difficulties were encountered in determining the thermal conductivity of the flat plate. It was known that the plate was made out of aluminum, likely of the 6000 series. However, the exact aluminum alloy used was not known, since it was never specified to the machine shop that created the flat plate. As a result, the material was chosen to have the same properties as 6061-T6 aluminum, a representative material

and a likely candidate. The thermal conductivity was determined from the reference literature to be 177 w/mK [8].

Several values were then calculated from the given input parameters. First, the speed of sound is needed to calculate the velocity of the flow. It was determined to be 433 m/s according to following formula from gas dynamics:

$$c = \sqrt{\gamma R T_s} \qquad \textbf{Equation 2.1}$$

The working fluid, air, was assumed to be a perfect gas with γ= 1.4 from [9]. The flow velocity then calculated using the Mach number and speed of sound:

$$V = Ma \cdot c \qquad \textbf{Equation 2.2}$$

Since the inlet pressure and Mach number were known, the outlet pressure was calculated from the subsonic gas dynamics tables of NACA report 1135. Moreover, the theoretical mass flow was calculated to be 3.66 kg/s from NACA 1135, Chart 1 [9].

2.3 Heat Transfer Theory

The flow of air over a flat plate in a wind tunnel closely resembles a forced convection situation. Therefore, Newton's Law of Cooling can be utilized along with other forced convection equations to obtain the theoretical flat plate heat transfer. Useful equations for carrying out the theoretical analysis include:

$q = \bar{h}(\Delta T)$ **Equation 2.3** **[10]**

$Re = \frac{\rho V L}{\mu}$ **Equation 2.4** **[10]**

$\overline{Nu} = 0.0296\left(Re^{\frac{4}{5}}\right)\left(Pr^{\frac{1}{3}}\right)$ **Equation 2.5a** **[10]**

$\overline{Nu} = 0.032\left(Re^{\frac{4}{5}}\right)(Pr^{0.43})$ **Equation 2.5b** **[8]**

$\bar{h} = \frac{(\overline{Nu})(k_{air})}{L}$ **Equation 2.6** **[10]**

The properties used for the calculation of heat transfer are shown below in Table 2.3.

Table 3: Heat Transfer Calculation Properties

ρ	Air Density	4.19 kg/m^3
L	Plate Length	0.289 m
μ	Dynamic Viscosity	2.26 E-5 kg/ms
Pr	Prandtl Number	0.70
k_{air}	Air Thermal Conductivity	0.0321 W/mK
ΔT	Temperature Difference	170 K

Equations 2.5a and 2.5b are variations on the Dittus-Boelter Correlation of the form $Nu = C\,(Re^{0.8})(Pr^n)$ [8]. With Equation 2.5a, the theoretical heat transfer is 186 kW/m^2, while Equation 2.5b yields a value of 195 kW/m^2. Equations 2.5a and 2.5b came from two different heat transfer texts, and both were calculated to give a range of theoretical heat transfer values. The numbers obtained from the theoretical calculations provide a reference point for the experimentally and computationally obtained values.

Chapter 3
COMPUTATIONAL FLUID DYNAMICS

3.1 Introduction

The FINE/Turbo software family handled all of the computational processes of this research, from grid generation and processing to post-processing. By keeping all computational activities within a single software package, the difficulties of moving from one platform to another were completely eliminated. All computations were carried out using a dual-core Intel Xenon processor, with each core running at a clock speed of 2.99 GHz. Although the GTL has a 16-node SGI cluster available for major computational activities, it could not be utilized for this project. A basic understanding of blocks in FINE/Turbo is required to why this was the case.

Two sets of CFD models were created for this project. The first model contained a single block (domain) of air, with boundary conditions defining the inlet, outlet, and the solid walls. Meanwhile, the second model contained two blocks: one of air and one for the solid flat plate. In the two block model a mixture of boundary conditions were defined.

FINE/Turbo assigns each block its own processor if available, while the master command script runs on a separate processor. Since at most two blocks were used in these calculations, a maximum of three processors could be utilized to solve the flow equations. However, in order to run each block on a separate processor the grid sizes must be approximately equal. For the CFD grids with both a block of air and a metal plate, this unfortunately was not the case because of the way IGG meshes grids. Thus, only two processors could be used to solve the computations of this experiment, which led to the use of a single dual-core computer.

3.2 Preprocessing: IGG

The first step towards the successful completion of any CFD analysis is the accurate modeling of the relevant geometry. In order to accomplish this, detailed dimensions of the SCF and flat plate were taken. In addition, the leading edge of the flow model was assumed to start at the boundary layer bleed plate. This plate resets the boundary layer upstream of the cooled flat plate, removing the preformed boundary layer. The exit of the model was set at the trailing edge of the flat plate vane piece. Final dimensions for the computational model are shown in Table 4 below.

Table 4: Numerical Model Dimensions

	Length (m)	Width (m)	Height (m)
Flat Plate	0.289	0.114	0.0237
Air Flow	0.289	0.114	0.0536

After the relevant geometry were drawn in IGG, the grid meshes were created. For the single block CFD model, a mesh of 129 x 129 x 129 grid points was used for a final size of 2,146,689 points. Meanwhile, for the two block CFD model each block contained 129 x 129 x 129 grid points, resulting in a final size of 4,293,378 points. The mesh sizes were deliberately chosen to enable the use of multigridding, a technique which greatly enhances the convergence of CFD models and provides for more accurate and robust solutions. In multigridding, a coarse grid with fewer points is solved first, and the results are used as the initial conditions for the next grid step. In the multigrid shown in Table 5, grid 1 would be solved first and used as the initial input to grid 2. Then, grid 2 would be solved and become the initial input to grid 3, and so on. Multigridding is a powerful technique which is essential to obtaining good CFD predictions.

Consequently, five multigrid levels were used in this research effort. After setting up the multigrids, the final step of grid generation was to define the solid and fluid blocks, if necessary. A dialogue window in the grid generation tab of IGG made this very easy to do.

Table 5: Multigrid Levels for 129 Points

Multigrid level	X Grid Points	Y Grid Points	Z Grid Points
1	2	2	2
2	3	3	3
3	5	5	5
4	9	9	9
5	17	17	17
6	33	33	33
7	65	65	65
8	129	129	129

Following grid generation, the next step in IGG was to define the boundary conditions for the wall type. In the single block, all of the exterior walls of the model were set as solid, and the inlet and outlet of the flow were defined as shown in Figure 6. In the two block model, all of the exterior walls were defined as solid, and the inlet and outlet were chosen only in the fluid domain, shown below in Figure 7. However, much difficulty was encountered in determining the boundary condition of the solid/fluid interface in the two block model. At first, full non-matching boundary conditions were applied to this interface. However, the conjugate heat transfer model does not work well with adiabatic and isothermal conditions imposed at the interface boundary, so the connected boundary condition was selected instead.

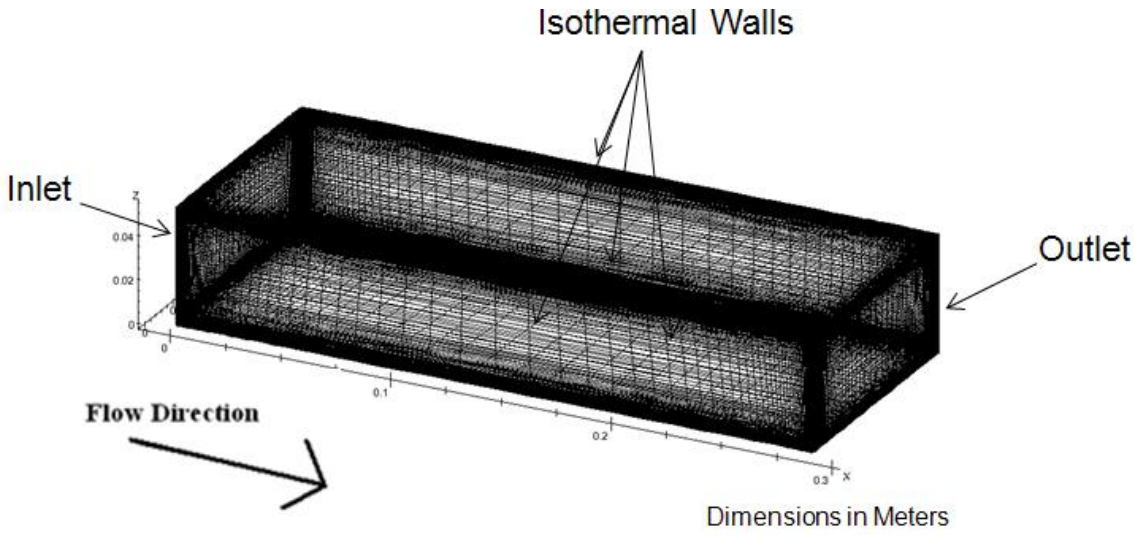

Figure 6: Single Block Wall Boundary Conditions

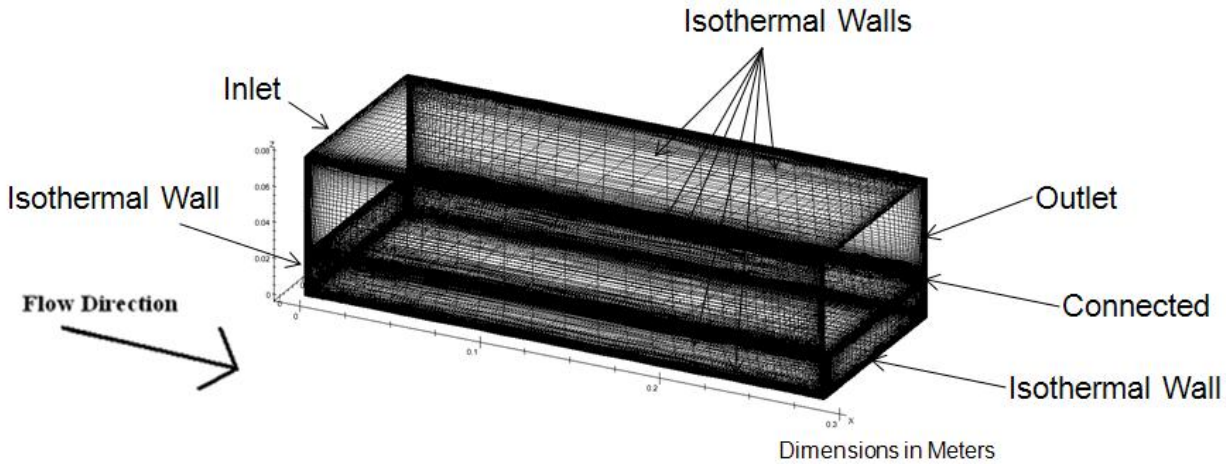

Figure 7: Two Block Wall Boundary Conditions

Once the boundary conditions were defined, the next task was to cluster grid points around the solid walls, the flow inlet, and the flow exit. Clustering points at these locations has the effect of reducing the y^+ values, improving computational stability. Moreover, clustering

around solid walls is absolutely necessary for accurately capturing the boundary layer. Clustering points around the inlet and exit allows for a more accurate computation of the mass flow, which is critical to verifying the final computational predictions.

The process of clustering points can be confusing and difficult. Through trial and error however, best practices were found. Using the "At Both Ends" option on each edge clusters grid points at the beginning and end of a given line segment. A proper clustering was achieved by repeating this step over all 12 edges in the single block mesh, and all 24 edges in the two block mesh. Clustering density values on the order of $3*10^{-6}$ were used to achieve good grid resolution around the walls.

The sensitivity of grid clustering was very important to the final stability of the mesh. For example, in one scenario only 23 of the 24 edges were clustered, with one edge mistakenly carrying evenly spaced grid points. The flow solver was unable to solve the grid, and the flow solution blew up. The problem was fixed simply by returning to IGG and clustering the final edge.

Before concluding the IGG mesh generation process, it was of paramount importance to check the overall quality of the mesh. The final product had a high percentage of orthagonality, and none of the cells were negative.

3.2 Preprocessing: Flow Parameters

After a finished mesh was created and the wall boundary conditions were defined, it was necessary to specify the flow parameters. A 3D Cartesian grid in meters was chosen in the main FINE/Turbo interface, the same as what was defined during the grid generation process.

For the turbulence model, the Spalart-Allmaras (S-A) model was selected due to its computational stability, fast convergence, and ease of use. Several other turbulence models exist as options in FINE/Turbo, including the less robust Baldwin-Lomax model and the more advanced k-epsilon models. However, the S-A model provides a good balance between the different models, and has been successfully used in the past at the GTL for FINE/Turbo simulations [11].

Proper specification of the flow parameters is one of the most critical steps in obtaining accurate CFD predictions. Even a small change in a single value can have a large effect on the final output. Static quantities were imposed at the air inlet, with a velocity of 173 m/s, a static temperature of 470K, and a turbulence viscosity of 0.0001 m^2/s. This value for the turbulence viscosity was left at its default. At the flow outlet, static pressure imposed boundary condition were selected and a constant pressure of 463.1 kPa was specified, per Table 3 in the previous chapter.

A five step multigrid was used for the numerical model. Additionally, the number of iterations per multigrid was increased in the expert parameters section of FINE/Turbo to help speed model convergence. An initial solution for the air domain was set using the same values as the input boundary conditions.

Cooling flow parameters were set in the main FINE/Turbo user interface. Five rows of injectors, totaling 113 cooling holes, were inserted into the mesh. Table 6 shows the location of the cooling holes, as well as other pertinent cooling geometry.

Table 6: Cooling Hole Location and Geometry

Row	Number of Holes	Distance from Leading Edge(mm)	Pitch (mm)	Diameter (mm)
1	16	86.36	2.438	0.457
2	15	88.27	2.540	0.457
3	33	91.64	1.219	0.305
4	32	108.03	1.143	0.406
5	17	113.13	0.965	0.356

After all boundary conditions, flow parameters, and cooling holes were defined, the flow solver was then started. As stated previously, only a single dual processor computer was used, which resulted in long computation times. For example, a typical two block mesh of 4,293,378 grid points and 2700 iterations required in excess of 24 hours to solve. This limited the number of CFD grids that could be run to two or three per week, greatly limiting the final number of computations. The computation time could have been reduced by using fewer grid points or less iterations, but this would have adversely affected the quality of the mesh. In fact, computation time was the single largest limiting factor of this research.

An important discovery was made while defining the boundary conditions of the solid walls. Initially adiabatic walls were defined, but it quickly became apparent that the solutions were highly dependent on the number of iterations. For example, after a run of 1000 iterations the adiabatic wall temperature would be one value, while after a run of 2000 iterations the wall temperature would be another value. Meanwhile, both runs would show convergence in terms of both global residual and mass flow. What mostly likely caused this phenomenon was using a steady, non time accurate flow solver, so that the number of iterations could be correlated to the length of the run of the experiment. Using more iterations caused the experiment to run longer, increasing the final temperature of the adiabatic walls.

To solve this problem, all of the solid walls were constrained to be isothermal (temperature imposed) at 300K. The actual experiment in the SCF will take only a matter of seconds, so the temperature of the walls is not expected to rise significantly above this value. Meanwhile, this will still permit a steady solution of the CFD mesh.

However, fixing the solid walls as isothermal at 300K only allowed for a solution of the single block mesh. For the two block case, the additional boundary between the solid and fluid needed to be defined. Initially adiabatic conditions were set at the interface, but like with the solid walls, an iteration problem was encountered. The first computation ran with 800 iterations, shown below in Figure 8. Although the solution appears to have mostly converged in the left side of the Figure 8, the right side shows a strong temperature gradient in the bottom solid block. In Figure 9, the solution finally looks completely converged at 3600 iterations. As in the previous case, however, a temperature gradient still exists in the block. It took the 9000 iterations of Figure 10 to completely solve the CFD mesh. The right side of Figure 10 shows a completely homogenous bottom solid block, which is to be expected for a steady adiabatic condition. Thus, it was learned that steady solutions exhibit strong iteration sensitivity with adiabatic conditions. Adiabatic boundary conditions should be used only with great caution when dealing with short and medium duration experiments such as this one.

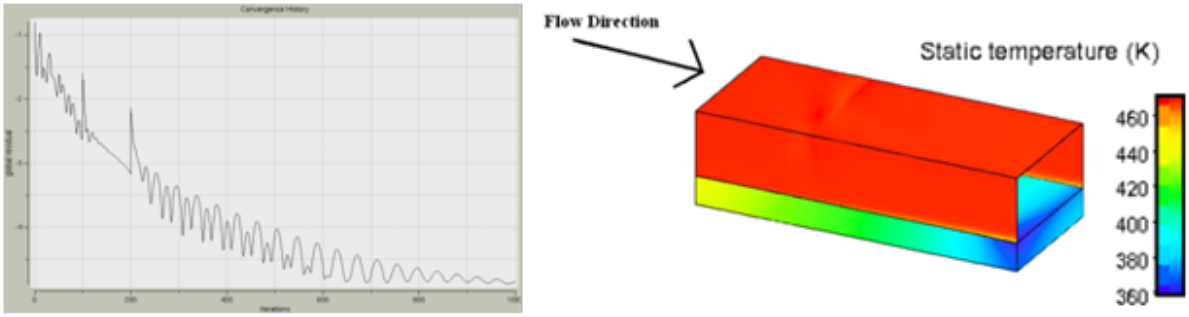

Figure 8: Flow Convergence at 800 Iterations

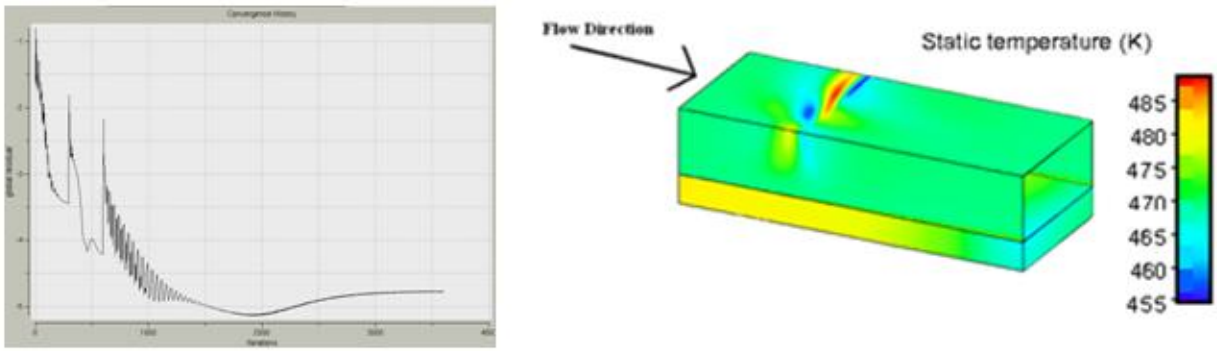

Figure 9: Flow Convergence at 3600 Iterations

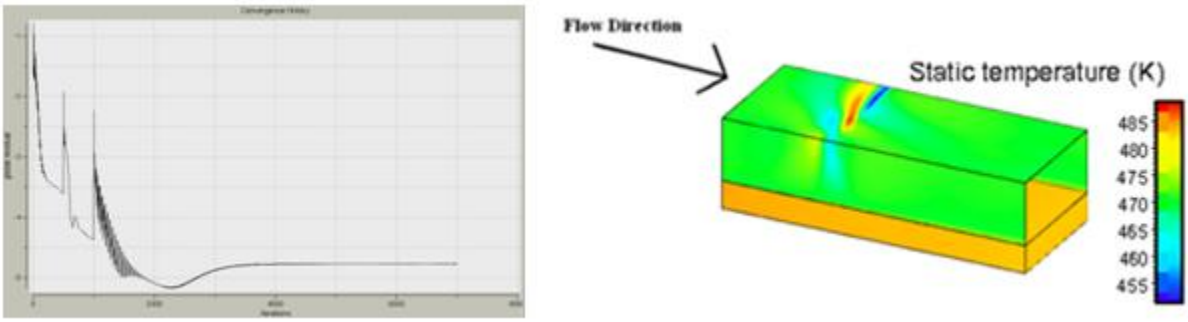

Figure 10: Flow Convergence at 9000 Iterations

The solutions of Figures 8 through 10 above also provided an important lesson on the use of fixed point clustering. In the mesh that was solved to create the CFD solutions above, a fixed point was added about 1/3 of the way downstream of the leading edge near the cooling holes. The fixed point was then gridded with a fine resolution, in order to better capture the cooling flow in the model. However, it was quickly discovered that the addition of this fixed point was causing strange behavior in the computation model. Even without cooling, unusual temperature spikes were predicted downstream of the leading edge. Figures 8 through 10 above show a model without cooling flow, yet there are temperature spikes at the fixed points. After much experimentation, the use of fixed points was deemed unnecessary and was abandoned in subsequent computation models.

Chapter 4
RESULTS AND DISCUSSION

4.1 Single Block Results

Although the single block CFD mesh was relatively simple in nature, it was still able to provide a useful prediction of flat plate heat transfer. Figure 11 shows a color map of the heat transfer for the single block case. Relevant boundary conditions from Tables 1 and 2 are repeated in Table 7 below for ease of reference.

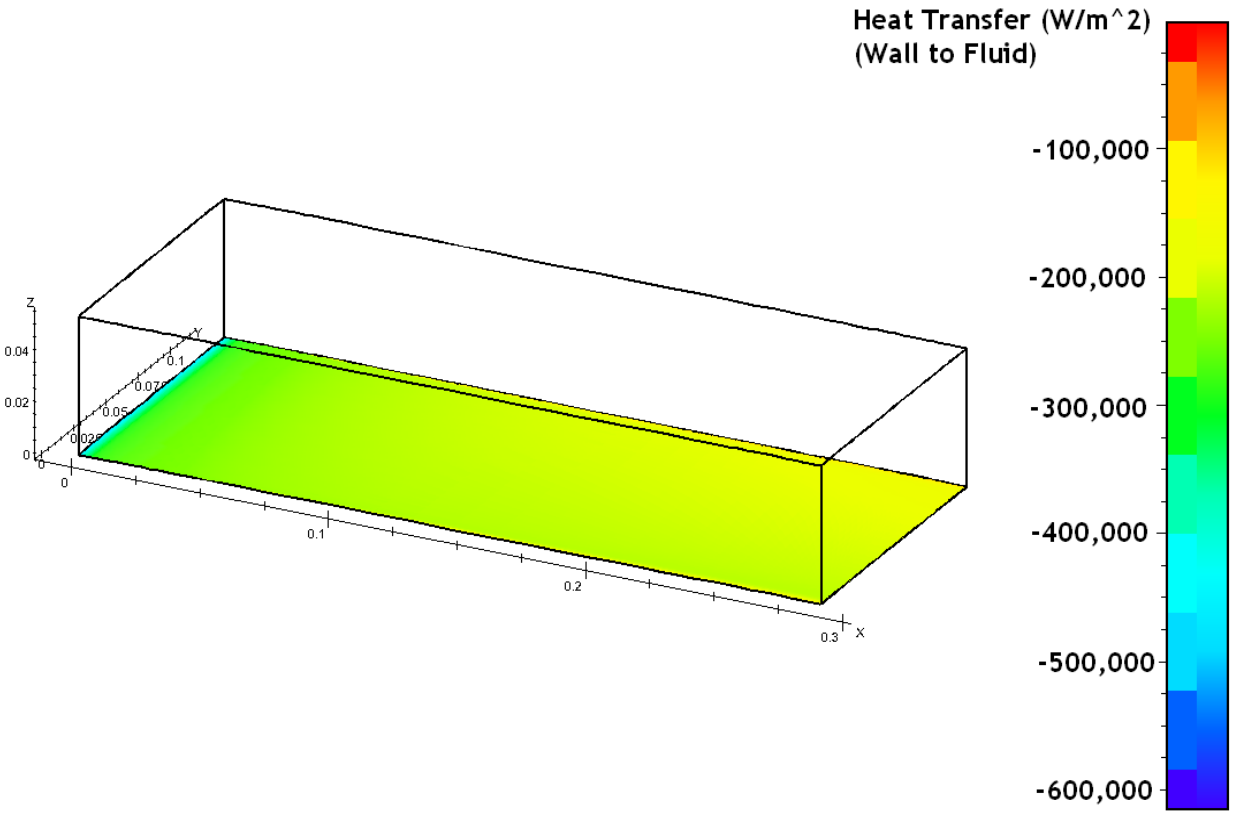

Figure 11: Uncooled Single Block Heat Transfer

Table 7: Single Block Flow Parameters

Ma	Inlet Mach Number	0.4
T_s	Inlet Static Temperature	470 K
V	Flow Velocity	173 m/s
Po	Outlet Pressure	463.13 kPa
T_{wall}	Wall Temperature	300 K
m_c	Cooling Mass Flow	0.006 kg/s
T_{cool}	Cooling Gas	240 K

The color scheme in Figure 11 is backwards from normal convention. All heat transfer predictions in FINE/Turbo are given from the wall to the fluid, so in cases where the gas is warmer than the wall a negative result is obtained. In this experiment, and in virtually every turbomachinery application, the main gas flow will be warmer than the walls, so a negative value will be predicted. This is a matter of nomenclature and does not affect the overall predictions.

Since the color scheme is backwards, the greatest heat transfer occurs in the blue regions (most negative) of Figure 11. As expected, the largest heat transfer is at the leading edge of the flat plate, since the boundary layer is thinnest there. As the boundary layer develops the heat transfer drops off rapidly, because the hot gas is unable to interact as strongly with the colder flat plate. A line of measurements was taken at the same location as the left side heat flux gauges on the experimental flat plate, shown below in Figure 12. A plot of heat transfer versus x-distance for the uncooled single domain flat plate is included below in Figure 13.

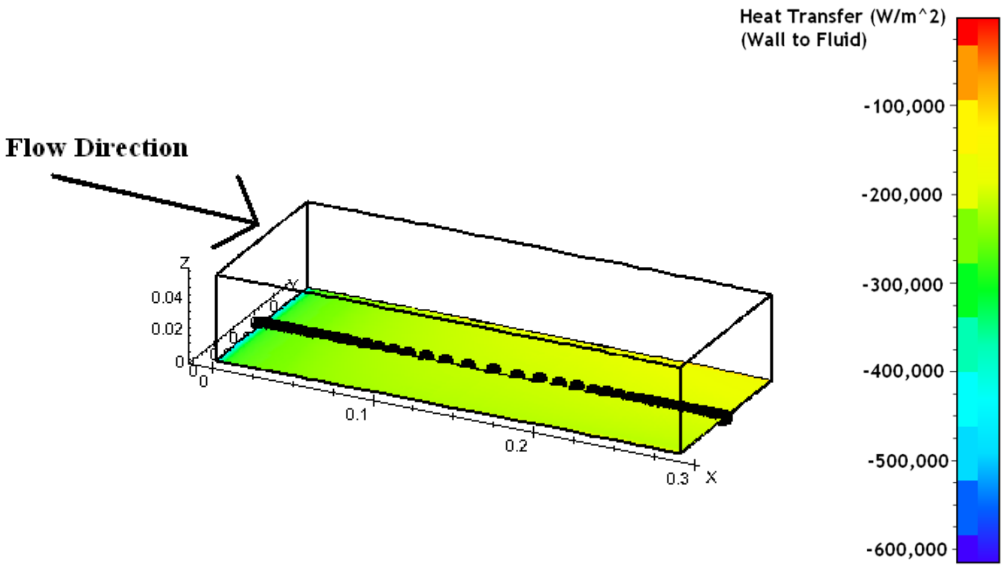

Figure 12: Uncooled Single Block Gage Location

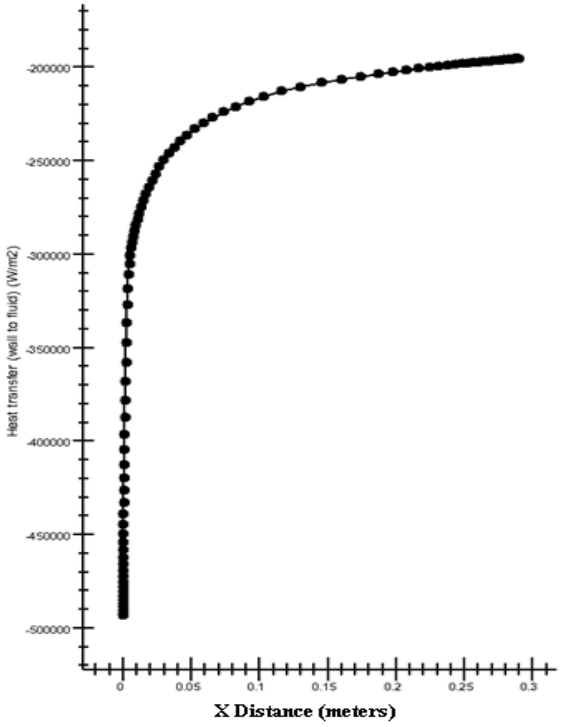

Figure 13: Uncooled Single Block Heat Transfer Graph

Figure 13 shows the greatest heat flux at the leading edge, in agreement with the color maps of Figures 11 and 12. The heat flux appears to reach an asymptotic value as the boundary layer fully develops. The lowest value of heat transfer was 196 kW/m^2 at the trailing edge. Meanwhile, the theoretical heat transfer from Equation 2.3 was 186 to 195 kW/m^2, in excellent agreement with the CFD predictions. The theoretical and predicted values compare well with each other, which helped to validate the computational model.

Comparing the theoretical and predicted mass flows also provided a check on the accuracy of the model. The equations and charts of NACA 1135 gave a theoretical mass flow of 3.66 kg/s, while the CFD predictions gave a mass flow of 3.64 kg/s. Again, these numbers are in close agreement and provided a basic check on the model.

After the uncooled single domain predictions were obtained, cooling flow was added to the model. Figure 14 below shows a color map of the single domain with cooling. The colors are again backwards from normal convention, with the greatest heat transfer occurring in the blue region and the least heat transfer in the red region. The addition of cooling holes significantly decreased the heat transfer both around and downstream of the cooling holes. Figure 15 shows a line of heat transfer predictions, and Figure 16 below is a plot of those points.

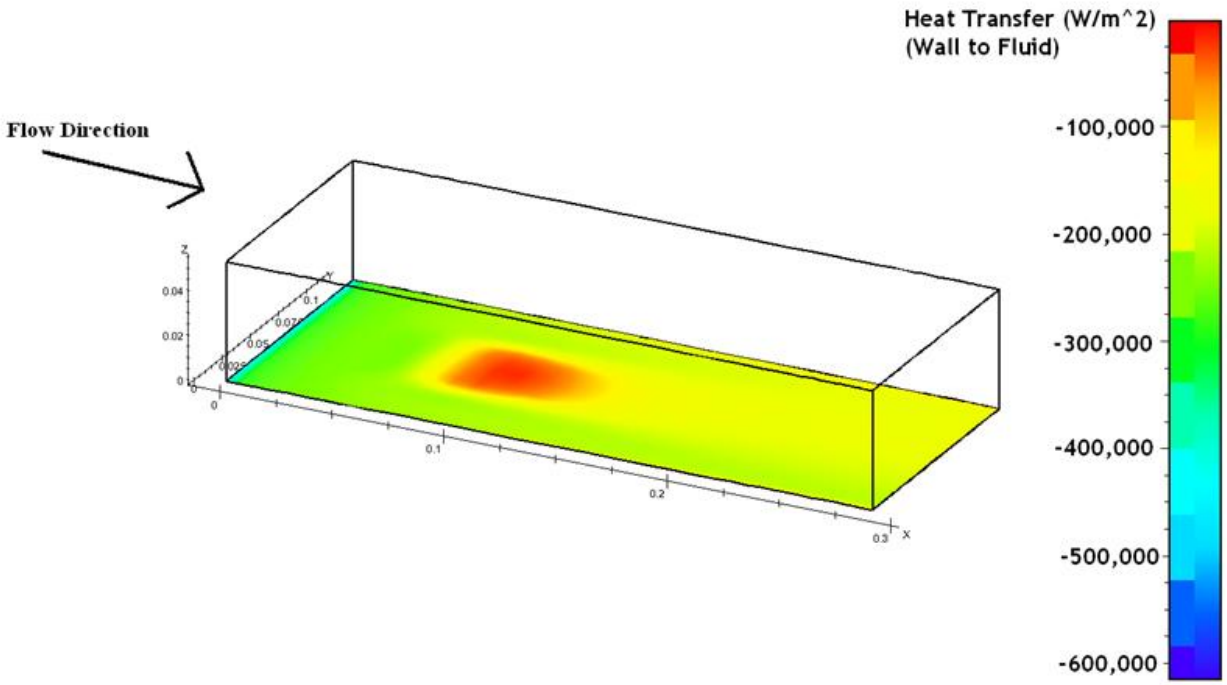

Figure 14: Cooled Single Block Heat Transfer

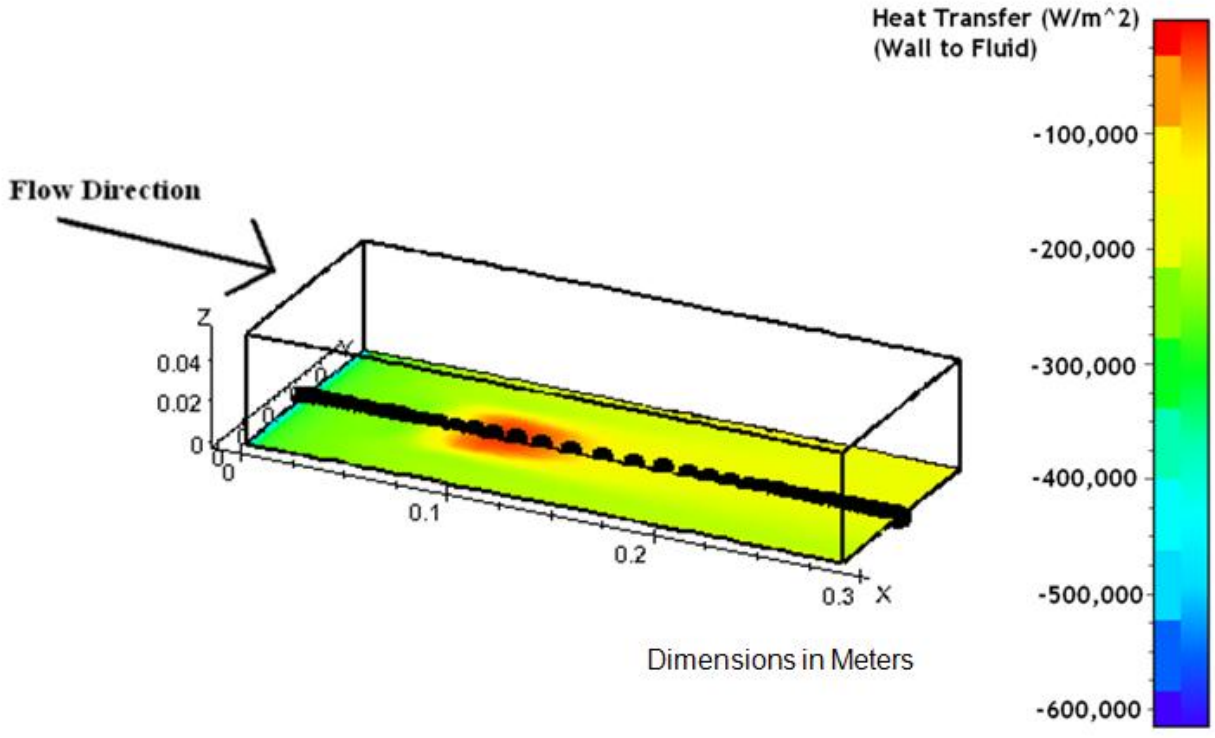

Figure 15: Cooled Single Block Gauge Location

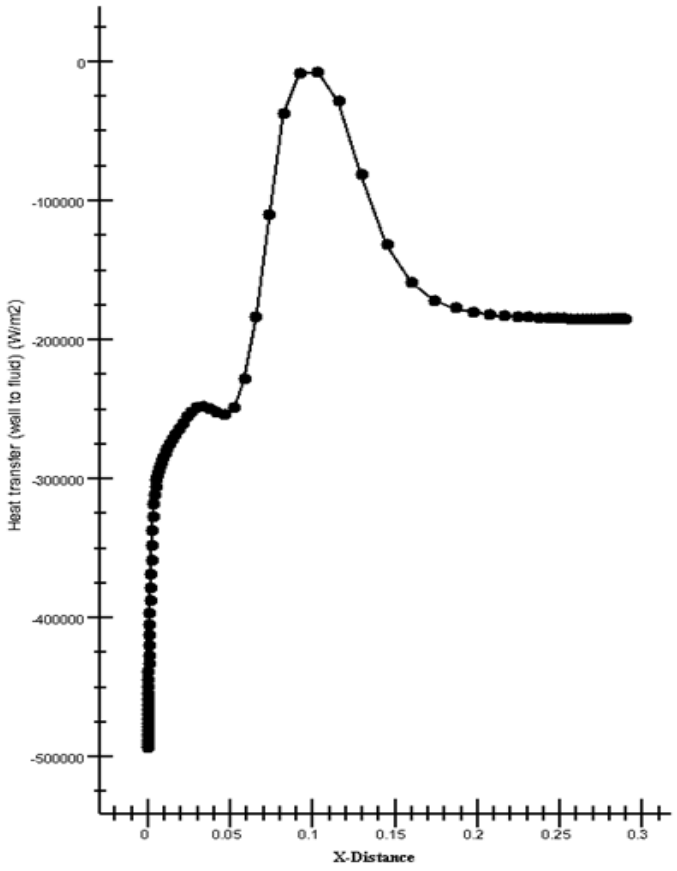

Figure 16: Cooled Single Block Heat Transfer Graph

Figure 16 dramatically shows the effect of cooling gas on flat plate heat transfer. In fact, the addition of cooling gas caused the heat transfer to drop to almost zero for a short section of the plate. As the cooling gas mixed with the main flow downstream, however, the heat transfer increased again and approached an asymptotic value. Figure 17 below compares the cooled and uncooled heat transfer predictions for the single block case.

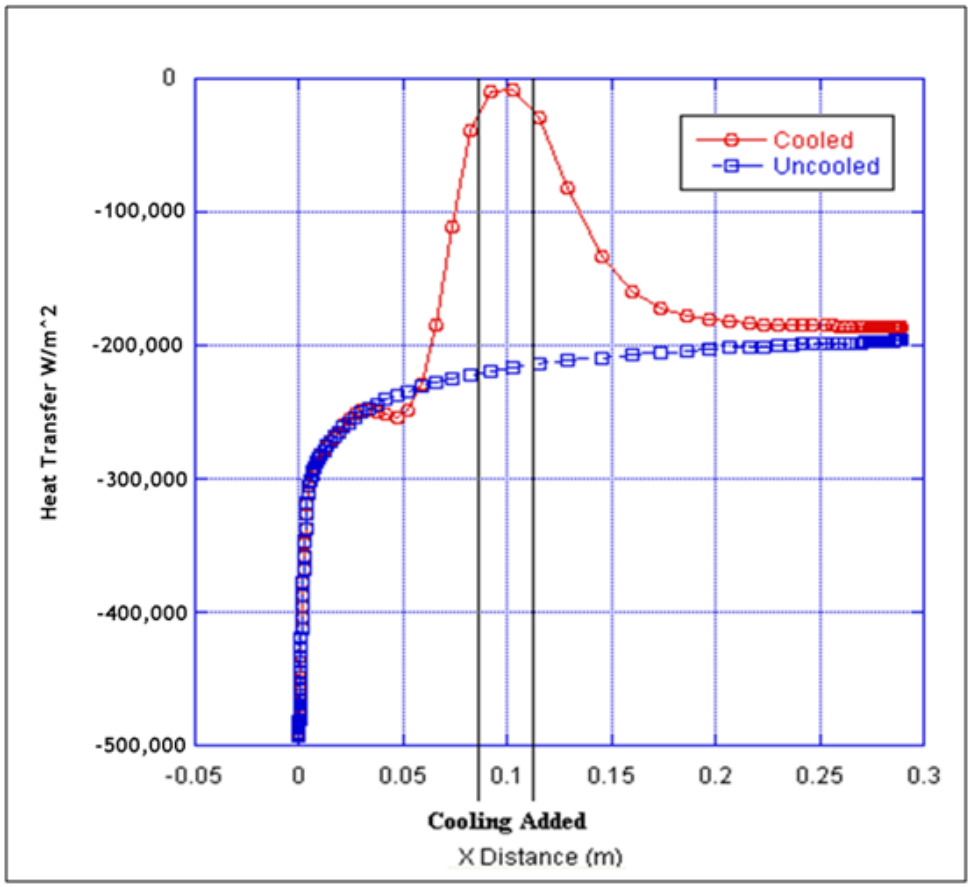

Figure 17: Comparison of Single Block Cooled and Uncooled Heat Transfer

The heat transfer is the same for both the cooled and uncooled plates upstream of the cooling holes, as expected. The addition of cooling gas has no effect on heat transfer at the leading edge. Moving downstream, adding cooling gas initially caused the heat transfer to increase before rapidly dropping off. The reason for this is uncertain. Additionally, this unusual result was obtained even when the mass flow of the cooling gas was increased by a factor of 5, so the behavior does not appear to be dependent on the amount of cooling mass flow.

Between the first and last row of cooling holes the CFD predictions gave a heat transfer value of almost zero. However, downstream of the cooling gas the heat transfer picked up again,

approaching the same asymptotic value as the uncooled flat plate. It is expected that with a long enough flat plate, the uncooled and cooled flat plate would reach the same heat transfer value.

4.2 Two Block Results

Unlike the single block case, good predictions were not obtained for the two block mesh. This issue was not with the complexity of the grid, but rather with the way FINE/Turbo is setup to run steady cases. As mentioned in the previous section, adiabatic wall conditions are iteration sensitive and cannot be used for short to medium duration experiments. To get around this, for the single and two block case all external walls were set to isothermal at 300K. However, the two block case had the additional boundary condition of the solid/fluid interface.

At first, Full Non-Matching conditions were set at the solid/fluid junction, with isothermal (300K) conditions on the bottom face and adiabatic conditions on meshing top face. It was reasoned that this set of boundary conditions should solve for a steady solution. However, it was quickly discovered that the FINE/Turbo flow solver simply will not start with these input parameters. An isothermal to adiabatic face is not permitted with Full Non-Matching boundary conditions.

The two block grid was then meshed again, this time with connected boundary conditions on the solid/fluid interface. The conjugate heat transfer module was activated in FINE/Turbo, and the boundary conditions were set by default to heat flux imposed and temperature imposed. However, since the goal was to obtain a heat flux value and not provide the software with one, this boundary conditions was changed to adiabatic. For these parameters no solution was obtained, as the flow solution blew up. Finally, the heat flux imposed condition was changed to temperature imposed, and the default temperature imposed condition was changed to adiabatic.

For these conditions a solution was obtained; however, no confidence should be placed in its predictions. Too many parameters were altered, and it appears that that the software could not accurately solve a problem of this type. An uncooled solution that was obtained for the two block condition is shown below in Figure 18. A line of measurements is shown in Figure 19, and a plot of the heat transfer is included below as Figure 20.

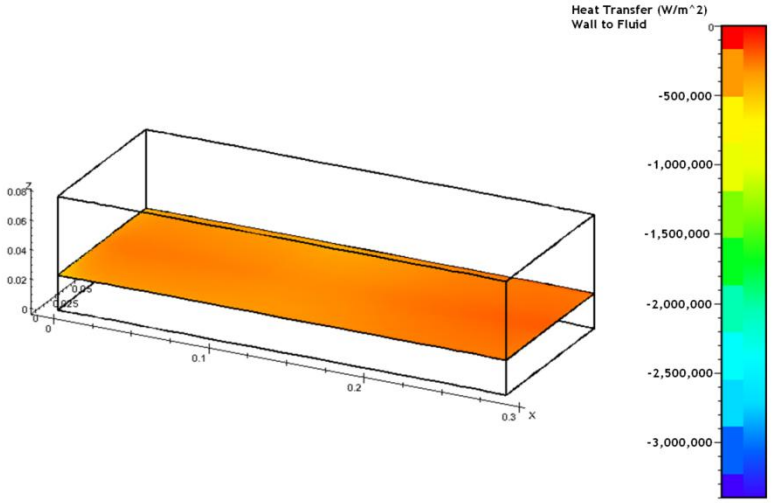

Figure 18: Uncooled Two Block Heat Transfer

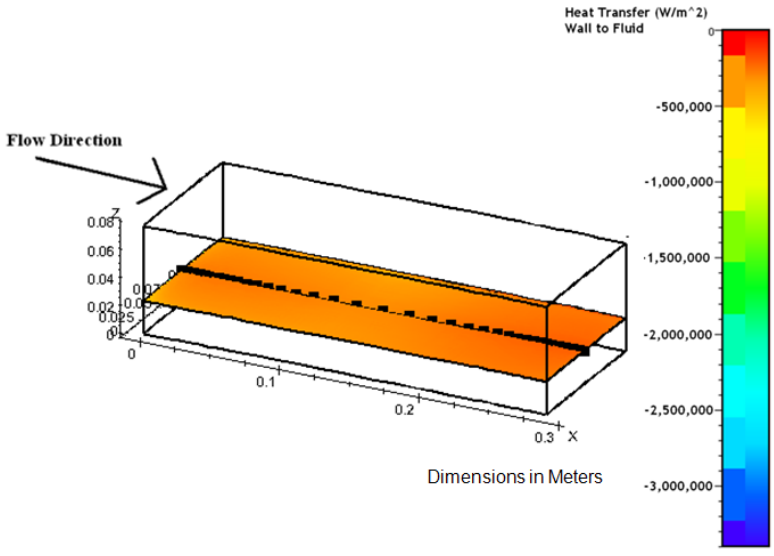

Figure 19: Uncooled Two Block Gauge Location

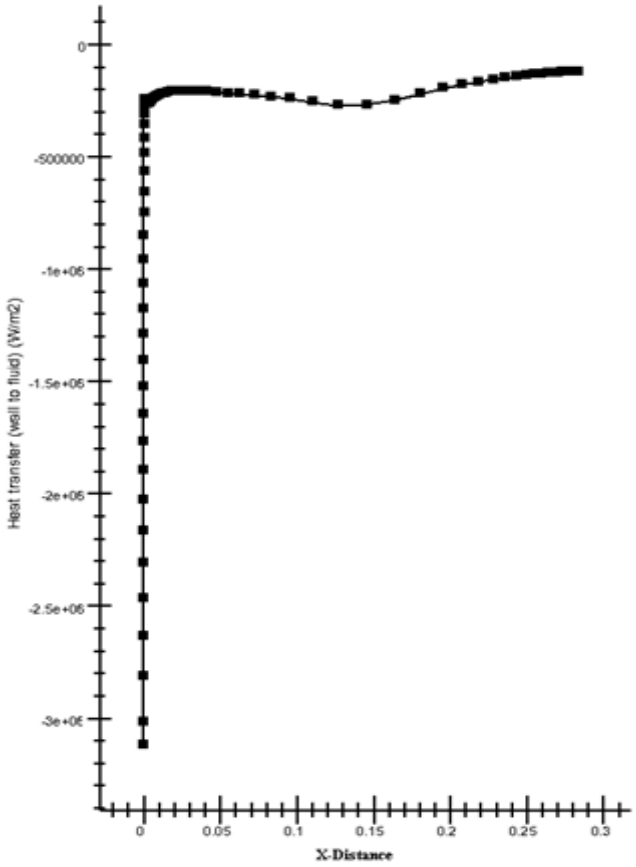

Figure 20: Uncooled Two Block Heat Transfer Graph

Figure 20 shows an extremely high heat transfer at the leading edge, which drops off rapidly with distance downstream. The boundary layer does not develop as with the single block predictions, which was much more reasonable solution. In sum, the two block heat transfer predictions were obtained in an unusual way and should not be considered accurate.

Chapter 5
CONCULSION

5.1 Final Statements

In conclusion, CFD predictions for the experimental flat plate were obtained in this research effort. Although experimental data is still in work and is unfortunately unavailable, computational predictions were compared with the theoretical value from forced convection heat transfer equations. The single block CFD model predicted a steady heat transfer of 196 kW/m^2 with a developed boundary layer. Since the theoretical value for a fully developed turbulent boundary layer was 186 to 195 kW/m^2, the CFD heat transfer predictions appear to be reasonable. Moreover, the single block mass flow of 3.64 kg/s compares well with the theoretical mass flow of 3.66 kg/s.

No reasonable CFD predictions were obtained for the two block grid. FINE/Turbo is unable to handle problems of this sort in the steady state, and a time accurate flow solver must be utilized in order to obtain heat transfer predictions. However, a time accurate flow solver was beyond the scope of this research project.

5.2 Lessons Learned

Caution is required when working in the steady state with adiabatic wall conditions, as solutions have been found to be highly iteration sensitive. Isothermal conditions are recommended for steady solutions, while a time accurate flow solver should be used to solve adiabatic conditions.

Clustering grid points around the inlet, outlet, and exterior walls of a mesh is crucial to obtaining accurate flow solutions. The clustering of points reduces the y^+ values and has a stabilizing effect on the mesh. It is important to cluster points around every external face and boundary, as missing just one spot can cause the flow solution to blow up. Additionally, the use of fixed points is not recommended, since they can cause unusual perturbations in the CFD predictions.

The heat transfer of the flat plate can be dramatically changed by the addition of cooling gas. Adding cooling gas has no affect far upstream of the injection holes, and far downstream of the cooling the heat transfer approaches the non-cooled asymptotic value. Essentially, the impact of cooling gas is limited to the region where it is added.

BIBLIOGRAPHY

[1] Dunn, M. G., 2001, "Convective Heat Transfer and Aerodynamics in Axial Flow Turbines," *ASME Journal of Turbomachinery,* Vol. 123, pp. 637-686.

[2] Haldeman, C. W., Mathison, R. M., Dunn, M. G., Southworth, S., Harral, J. W., and Heitland, G., 2006, "Aerodynamic and Heat Flux Measurements in a Single Stage Fully Cooled Turbine- Part I: Experimental Approach," ASME Paper No. GT2006-90966.

[3] Haldeman, C. W. and Dunn, M. G., 2003, "Heat Transfer Measurements and Predictions for the Vane and Blade of a Rotating High-Pressure Turbine Stage," ASME Paper No. GT2003-38726.

[4] Varadarajan, K. and Bogard, D. G., 2004, "Effects of Hot Streaks on Adiabatic Effectiveness for a Film Cooled Turbine Vane," ASME Paper No. GT2004-54016.

[5] Bernasconi, S. L., 2007, "Design, Instrumentation and Study on a New Test Section for Turbulence and Film Effectiveness Research in a Blowdown Facility". M.S. Thesis, ETH Zurich.

[6] Ou, S. and Rivir, R. B., 2006, "Shaped-Hole Film Cooling With Pulsed Secondary Flow," ASME Paper No. GT2006-90272.

[7] Giang, T. T. L., 1999, "Effects of Unsteady Cooling Flow on Heat Transfer to a Film-Cooled Flat Plate," M.S. Thesis, The Ohio State University.

[8] Lienhard, J. H. and Lienhard, J. H., 2008, *A Heat Transfer Textbook,* Cambridge, MA: Phlogiston Press.

[9] Anon., 1953, "Equations, Tables, and Charts for Compressible Flow," NACA rept. 1135.

[10] Incropera F.P. and DeWitt, D. P., 2002, *Fundamentals of Heat and Mass Transfer,* New York: Wiley.

[11] Crosh, E. A., 2008, “Time-Accurate Predictions for the Aerodynamics of a 1 and ½ Stage HP Transonic Turbine,” M.S. Thesis, The Ohio State University.